Supplementary Information

Hysteresis metrics reveal land-use-dependent stormflow constituent dynamics in tropical Afromontane catchments

Zadoki Tabo[1,2], Suzanne R. Jacobs[1,2], Lutz Breuer[1,2]

Affiliations

[1] Institute for Landscape Ecology and Resources Management (ILR), Research Centre for BioSystems, Land Use and Nutrition (iFZ), Justus Liebig University Giessen, Heinrich-Buff-Ring 26, 35392 Giessen, Germany

[2] Centre for International Development and Environmental Research (ZEU), Justus Liebig University Giessen, Senckenbergstrasse 3, 35390 Giessen, Germany

Contents

Table S1. Nested event populations and time-integrated chemical status 2-3

Table S2. Hysteresis limb dominance, pathway complexity, and loop structure 3

Figure S1. Initial storm discharge and hysteresis-index distributions 4

Figure S2. Initial-flow conditions of the analytical event subset 5

Figure S3. Integrated storm-event response patterns and hydrological context 6

Figure S4. PAM response-group selection and stability diagnostics 7

Figure S5. Hydrological distributions across response groups 8

Table S1. Nested event populations and time-integrated chemical status by catchment and solute.

Site/scale	Solute	All n	Nonresponsive n (% all)	Responsive n (% all)	Geometry n (% all)	All-event C/M/D, n (%)	All dominant	Responsive C/M/D, n (%)	Responsive dominant	Response class
All catchments	DOC	599	108 (18.0%)	491 (82.0%)	442 (73.8%)	C 398 (66.4%); M 187 (31.2%); D 14 (2.3%)	Chemostasis	C 290 (59.1%); M 187 (38.1%); D 14 (2.9%)	Chemostasis	Pooled
All catchments	EC	675	574 (85.0%)	101 (15.0%)	88 (13.0%)	C 658 (97.5%); M 11 (1.6%); D 6 (0.9%)	Chemostasis	C 84 (83.2%); M 11 (10.9%); D 6 (5.9%)	Chemostasis	Pooled
All catchments	NO_3–N	629	345 (54.8%)	284 (45.2%)	255 (40.5%)	C 561 (89.2%); M 61 (9.7%); D 7 (1.1%)	Chemostasis	C 216 (76.1%); M 61 (21.5%); D 7 (2.5%)	Chemostasis	Pooled
All catchments	TSS	603	7 (1.2%)	596 (98.8%)	538 (89.2%)	C 147 (24.4%); M 417 (69.2%); D 39 (6.5%)	Mobilization	C 140 (23.5%); M 417 (70.0%); D 39 (6.5%)	Mobilization	Pooled
NF	DOC	249	85 (34.1%)	164 (65.9%)	146 (58.6%)	C 186 (74.7%); M 61 (24.5%); D 2 (0.8%)	Chemostasis	C 101 (61.6%); M 61 (37.2%); D 2 (1.2%)	Chemostasis	Intermediate response
NF	EC	278	251 (90.3%)	27 (9.7%)	25 (9.0%)	C 275 (98.9%); M 3 (1.1%); D 0 (0.0%)	Chemostasis	C 24 (88.9%); M 3 (11.1%); D 0 (0.0%)	Chemostasis	Low response
NF	NO_3–N	250	150 (60.0%)	100 (40.0%)	93 (37.2%)	C 225 (90.0%); M 25 (10.0%); D 0 (0.0%)	Chemostasis	C 75 (75.0%); M 25 (25.0%); D 0 (0.0%)	Chemostasis	Intermediate response
NF	TSS	245	5 (2.0%)	240 (98.0%)	214 (87.3%)	C 85 (34.7%); M 153 (62.4%); D 7 (2.9%)	Mobilization	C 80 (33.3%); M 153 (63.8%); D 7 (2.9%)	Mobilization	High response
SHA	DOC	158	16 (10.1%)	142 (89.9%)	132 (83.5%)	C 126 (79.7%); M 23 (14.6%); D 9 (5.7%)	Chemostasis	C 110 (77.5%); M 23 (16.2%); D 9 (6.3%)	Chemostasis	Intermediate response
SHA	EC	171	132 (77.2%)	39 (22.8%)	32 (18.7%)	C 163 (95.3%); M 3 (1.8%); D 5 (2.9%)	Chemostasis	C 31 (79.5%); M 3 (7.7%); D 5 (12.8%)	Chemostasis	Low response
SHA	NO_3–N	168	78 (46.4%)	90 (53.6%)	78 (46.4%)	C 152 (90.5%); M 12 (7.1%); D 4 (2.4%)	Chemostasis	C 74 (82.2%); M 12 (13.3%); D 4 (4.4%)	Chemostasis	Intermediate response
SHA	TSS	169	2 (1.2%)	167 (98.8%)	153 (90.5%)	C 29 (17.2%); M 121 (71.6%); D 19 (11.2%)	Mobilization	C 27 (16.2%); M 121 (72.5%); D 19 (11.4%)	Mobilization	High response
TTP	DOC	192	7 (3.6%)	185 (96.4%)	164 (85.4%)	C 86 (44.8%); M 103 (53.6%); D 3 (1.6%)	Mobilization	C 79 (42.7%); M 103 (55.7%); D 3 (1.6%)	Mobilization	High response
TTP	EC	226	191 (84.5%)	35 (15.5%)	31 (13.7%)	C 220 (97.3%); M 5 (2.2%); D 1 (0.4%)	Chemostasis	C 29 (82.9%); M 5 (14.3%); D 1 (2.9%)	Chemostasis	Low response
TTP	NO_3–N	211	117 (55.5%)	94 (44.5%)	84 (39.8%)	C 184 (87.2%); M 24 (11.4%); D 3 (1.4%)	Chemostasis	C 67 (71.3%); M 24 (25.5%); D 3 (3.2%)	Chemostasis	Intermediate response

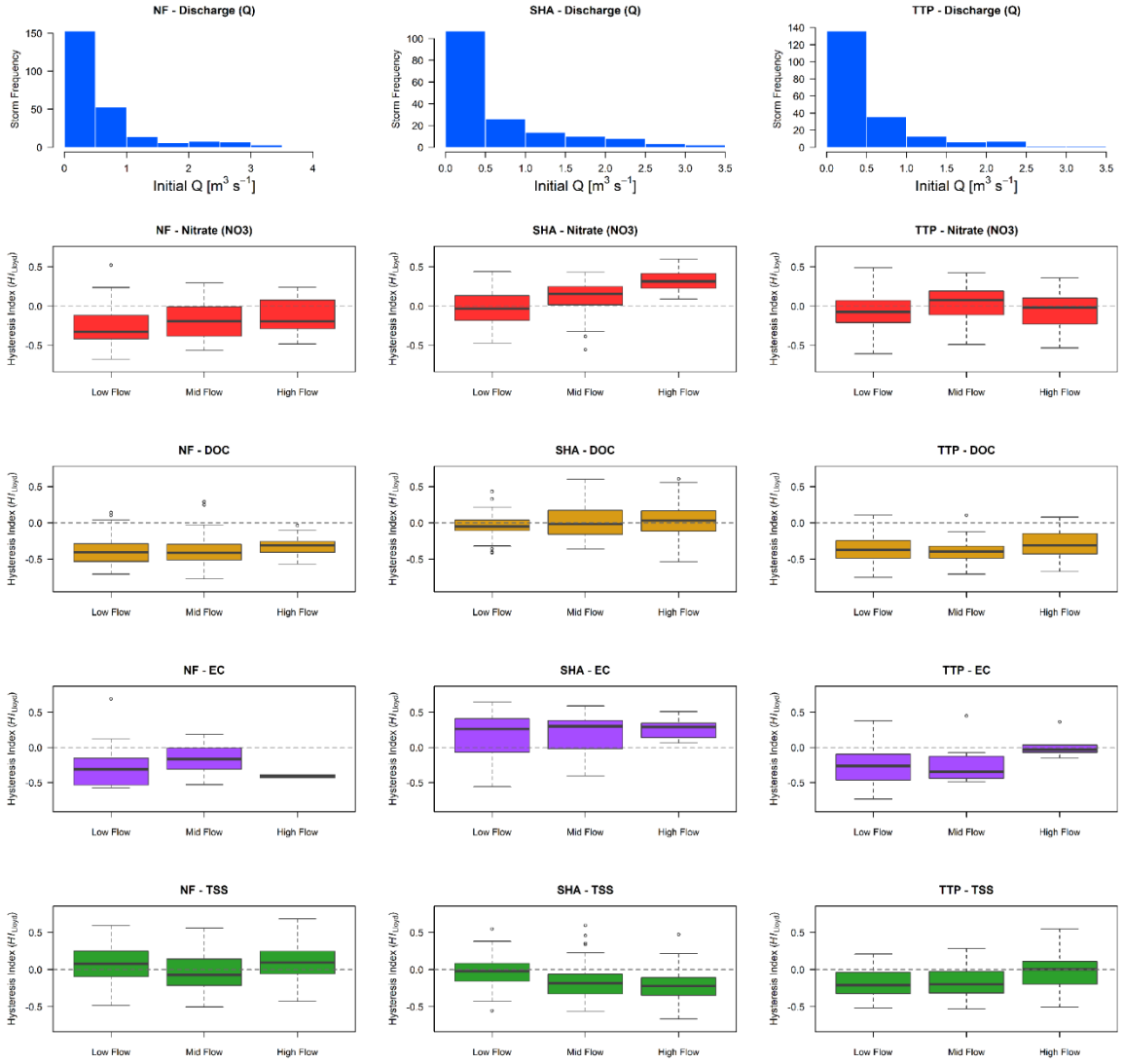
Site/scale	Solute	All n	Nonresponsive n (% all)	Responsive n (% all)	Geometry n (% all)	All-event C/M/D, n (%)	All dominant	Responsive C/M/D, n (%)	Responsive dominant	Response class
TTP	TSS	189	0 (0.0%)	189 (100.0%)	171 (90.5%)	C 33 (17.5%); M 143 (75.7%); D 13 (6.9%)	Mobilization	C 33 (17.5%); M 143 (75.7%); D 13 (6.9%)	Mobilization	High response

Note. C = chemostasis, M = mobilization, and D = dilution. All classifiable records have sufficient data, a valid C_0, and a time-integrated status. Responsive records contain at least one ±15% threshold excursion; geometry-resolved records additionally have finite HI_Lloyd, finite A_{loop}, and a valid loop class. A responsive event can remain time-integrated chemostatic when the excursion is brief. The pooled rows provide the overall classifiable-population status totals.

Table S2. Hysteresis limb dominance, pathway complexity, and loop structure for responsive, geometry-resolved event–constituent combinations.

Site	Solute	n	HILloyd median (mean)	HILloyd +/−/≈0 (%)	Aloop median (mean)	Limb dominance	Complexity	Dominant loop, n (%)	Secondary loop, n (%)	Versus NF
NF	DOC	146	-0.402 (-0.377)	2.7/95.2/2.1	0.382 (0.384)	Falling-limb dominant	High	Anticlockwise: 103 (70.5%)	Figure-8/mixed: 43 (29.5%)	Reference
NF	EC	25	-0.292 (-0.227)	12.0/76.0/12.0	0.312 (0.349)	Falling-limb dominant	High	Anticlockwise: 13 (52.0%)	Figure-8/mixed: 11 (44.0%)	Reference
NF	NO_3–N	93	-0.295 (-0.224)	14.0/76.3/9.7	0.306 (0.311)	Falling-limb dominant	Moderate	Figure-8/mixed: 57 (61.3%)	Anticlockwise: 35 (37.6%)	Reference
NF	TSS	214	0.041 (0.043)	48.6/36.4/15.0	0.203 (0.229)	Balanced/mixed	Low	Figure-8/mixed: 141 (65.9%)	Clockwise: 42 (19.6%)	Reference
SHA	DOC	132	-0.016 (-0.002)	37.1/39.4/23.5	0.203 (0.226)	Balanced/mixed	Low	Figure-8/mixed: 115 (87.1%)	Anticlockwise: 10 (7.6%)	Lower than NF
SHA	EC	32	0.264 (0.179)	75.0/21.9/3.1	0.302 (0.302)	Rising-limb dominant	Moderate	Clockwise: 15 (46.9%)	Figure-8/mixed: 14 (43.8%)	Similar to NF
SHA	NO_3–N	78	0.115 (0.095)	60.3/24.4/15.4	0.233 (0.260)	Rising-limb dominant	Moderate	Figure-8/mixed: 50 (64.1%)	Clockwise: 21 (26.9%)	Similar to NF
SHA	TSS	153	-0.144 (-0.140)	19.6/69.9/10.5	0.245 (0.257)	Falling-limb dominant	Moderate	Figure-8/mixed: 111 (72.5%)	Anticlockwise: 33 (21.6%)	Similar to NF
TTP	DOC	164	-0.366 (-0.355)	1.8/96.3/1.8	0.339 (0.351)	Falling-limb dominant	High	Anticlockwise: 102 (62.2%)	Figure-8/mixed: 61 (37.2%)	Similar to NF
TTP	EC	31	-0.161 (-0.172)	12.9/71.0/16.1	0.321 (0.275)	Falling-limb dominant	High	Figure-8/mixed: 16 (51.6%)	Anticlockwise: 12 (38.7%)	Similar to NF
TTP	NO_3–N	84	-0.031 (-0.046)	32.1/46.4/21.4	0.203 (0.227)	Balanced/mixed	Low	Figure-8/mixed: 61 (72.6%)	Anticlockwise: 15 (17.9%)	Lower than NF
TTP	TSS	171	-0.157 (-0.131)	21.1/63.7/15.2	0.207 (0.226)	Falling-limb dominant	Low	Figure-8/mixed: 124 (72.5%)	Anticlockwise: 42 (24.6%)	Similar to NF

Note. HI_Lloyd > 0 indicates rising-limb dominance and HI_Lloyd < 0 indicates falling-limb dominance; ≈0 denotes |HI_Lloyd| ≤ 0.05. These descriptors refer to relative concentrations on the two hydrograph limbs at equivalent discharge and do not, by themselves, uniquely identify source timing or pathway. A_loop is the normalized absolute area separating the rising and falling limbs. Pathway-complexity classes use the 33rd and 66th percentiles of the 12 site–constituent median loop areas (0.22395 and 0.30808). Values are based on the geometry-resolved populations and are the statistics underlying Figure 3b.



50

Figure S1. Empirical distributions of initial storm discharge (top row) and constituent-specific Lloyd hysteresis indices (HI Lloyd; rows 2–5), stratified by low-, mid-, and high-flow classes across the natural forest (NF), smallholder agriculture (SHA), and tea/tree plantation (TTP) catchments.

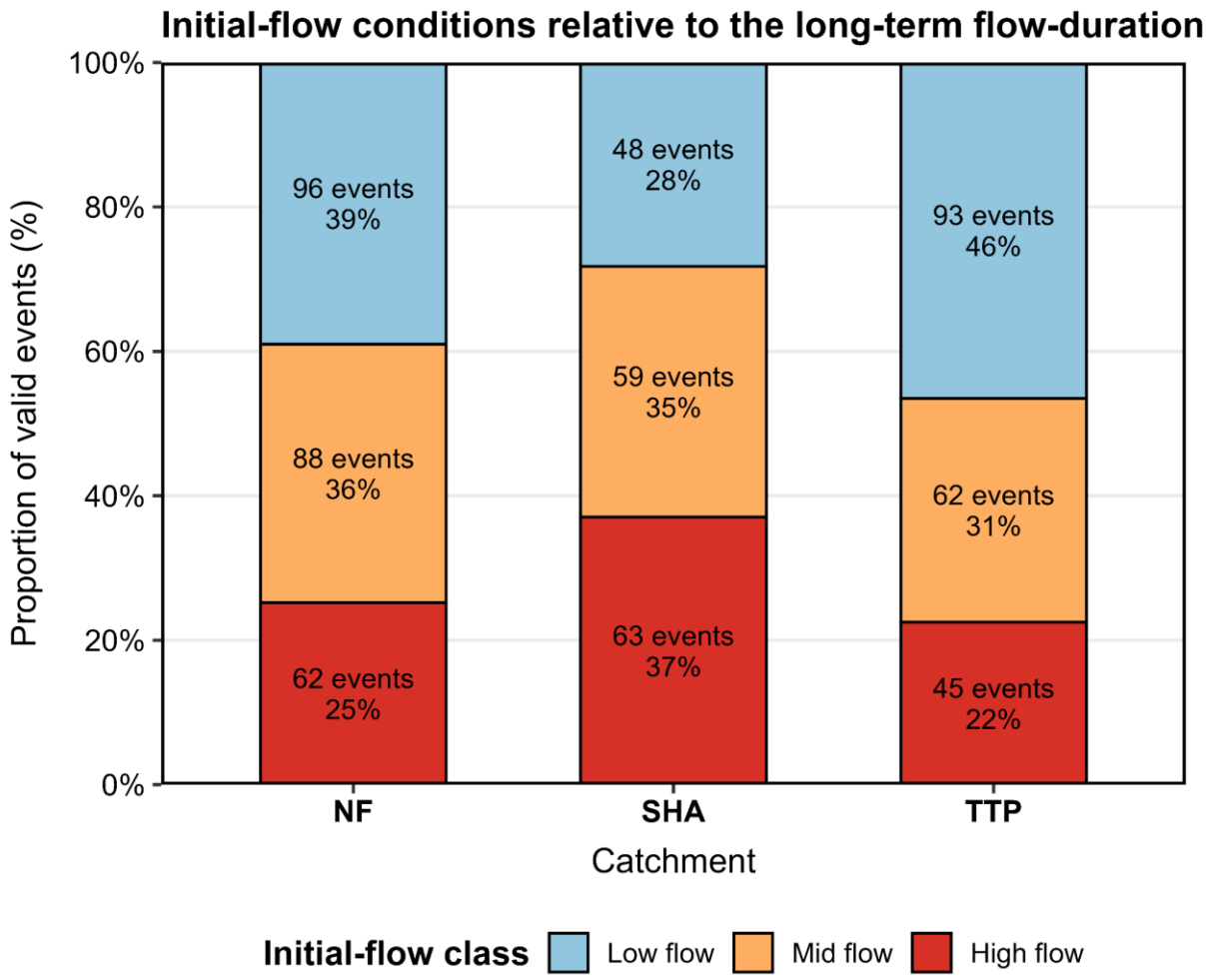


Figure S2. Initial-flow conditions of the event subset used for initial-flow analysis across the natural forest (NF), smallholder agriculture (SHA), and tea/tree plantation (TTP) catchments. Stacked bars show the proportion and number of valid events beginning under low-, mid-, and high-flow conditions, defined from the 33rd and 66th percentiles of each catchment's six-year daily discharge record.

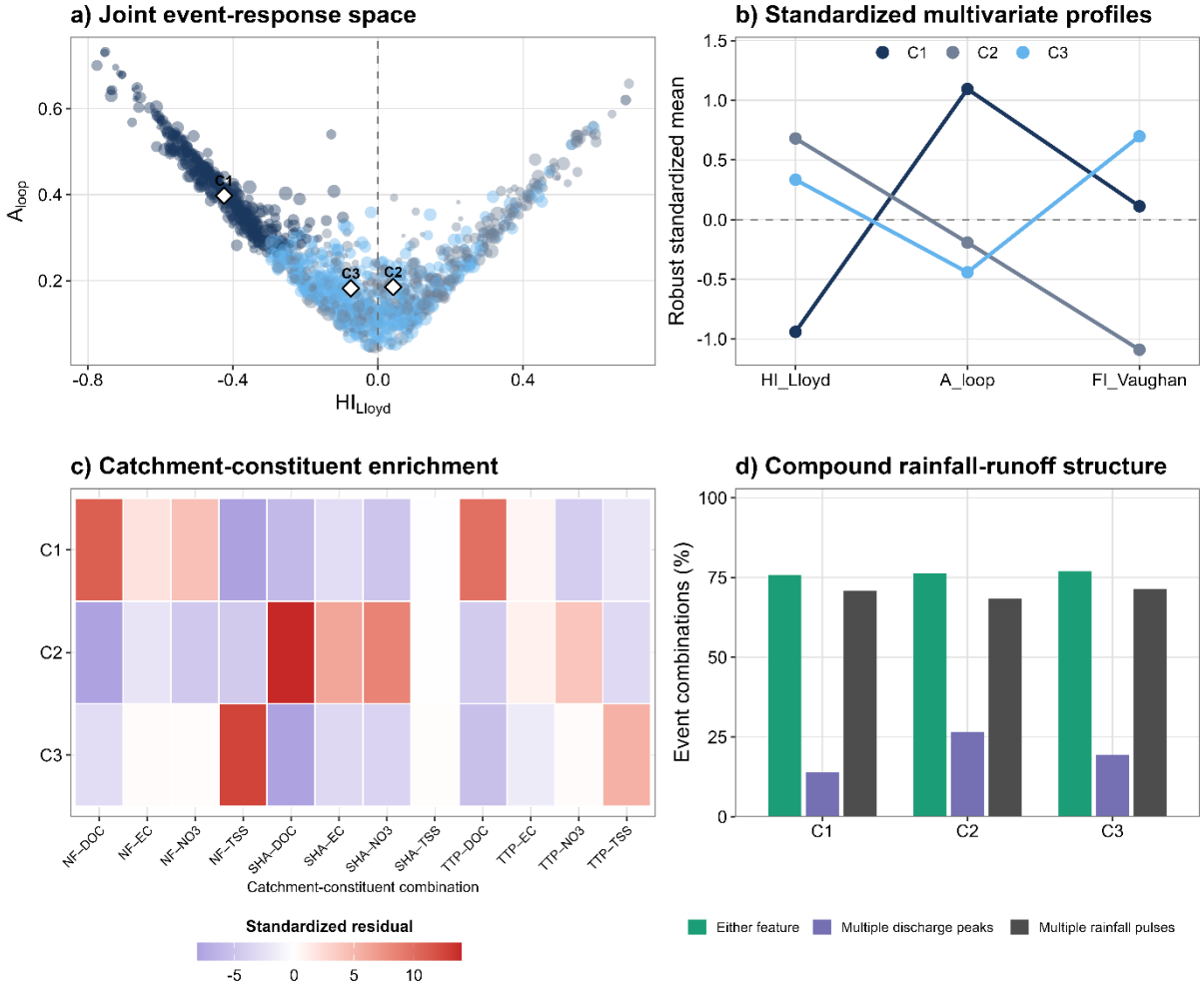


Figure S3.

Integrated storm-event response patterns and their hydrological context. (a) Joint HI_Lloyd–A_loop response space for the 1,319 responsive, geometry-resolved event–constituent combinations with finite Vaughan FI used in clustering; colours indicate PAM response group, point size represents |FI|, and labelled diamonds identify PAM medoids. (b) Robustly standardized mean profiles of HI Lloyd, A loop, and Vaughan FI for C1, C2, and C3. (c) Catchment–constituent enrichment expressed as adjusted standardized residuals from the response-group-by-catchment–constituent contingency table; positive values indicate combinations occurring more frequently than expected and negative values indicate depletion. (d) Percentages of combinations associated with multiple rainfall pulses, multiple discharge peaks, or either feature. The selected PAM solution had k = 3, an average silhouette width of 0.350, and mean bootstrap–Jaccard similarities of 0.946, 0.913, and 0.884 for C1, C2, and C3, respectively.

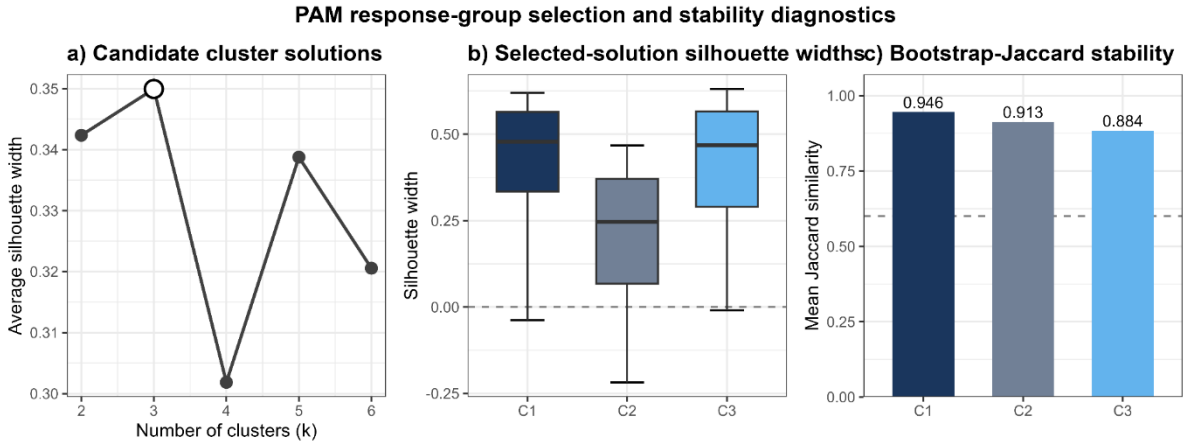


Figure S4. Partitioning-around-medoids (PAM) response-group selection and stability diagnostics. (a) Average silhouette width for candidate PAM solutions with k = 2–6; the open symbol identifies the selected k = 3 solution with average silhouette width 0.350. (b) Distribution of silhouette widths for observations assigned to C1, C2, and C3 in the selected solution; values below zero indicate observations lying closer to another response group than to their assigned group. (c) Mean bootstrap–Jaccard similarities for C1, C2, and C3 based on 200 resampling replicates. The dashed horizontal line denotes the operational stability criterion of 0.60. Mean Jaccard similarities were 0.946, 0.913, and 0.884 for C1, C2, and C3, respectively.

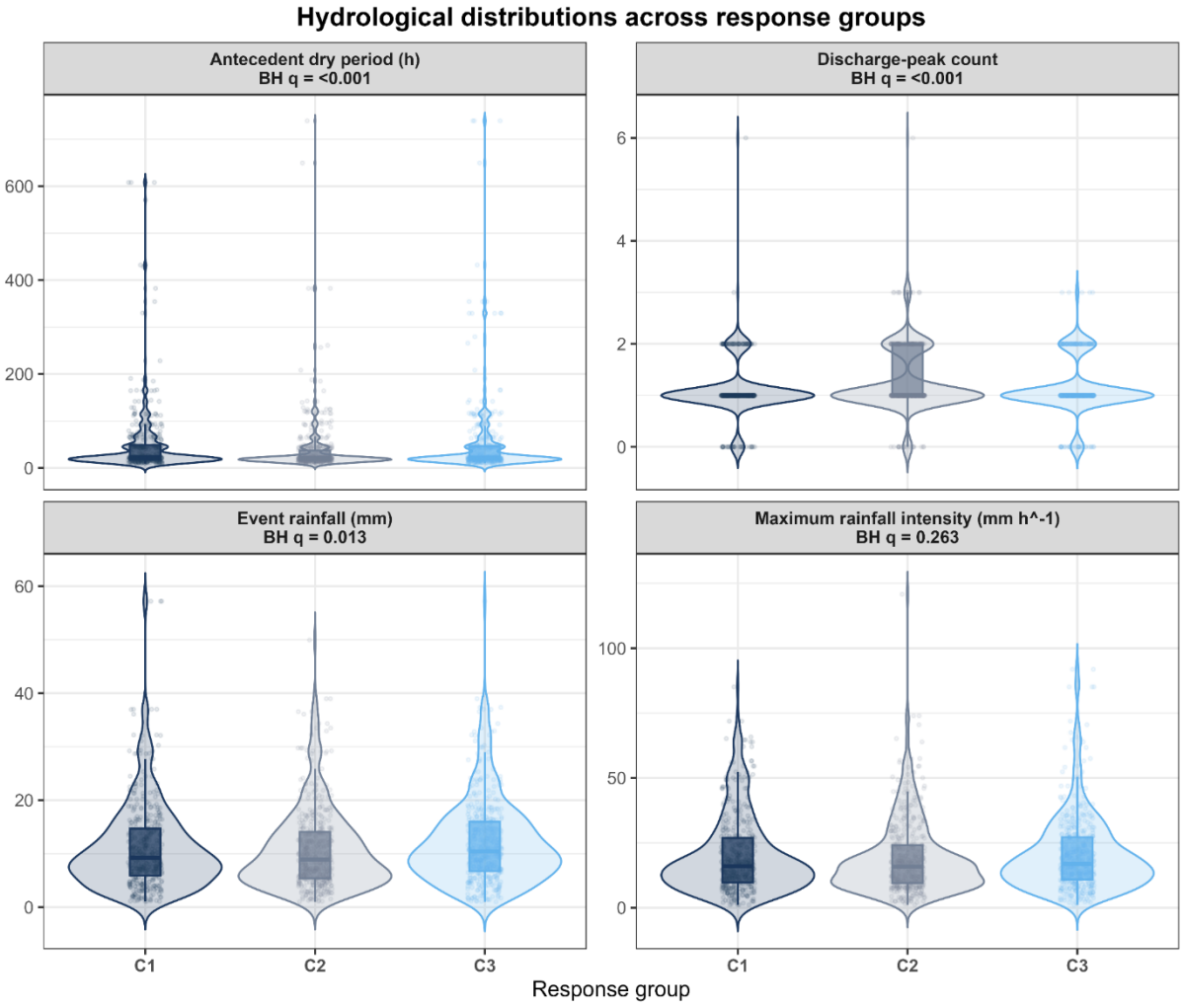


Figure S5. Hydrological distributions across the three multivariate response groups. Violin plots show antecedent dry period, discharge-peak count, event rainfall, and maximum rainfall intensity for C1, C2, and C3; embedded boxplots show medians and interquartile ranges, and semi-transparent points represent individual event–constituent combinations. Benjamini–Hochberg-adjusted Kruskal–Wallis q-values are shown above each panel. Antecedent dry period and discharge-peak count differed among groups at $q < 0.001$, event rainfall differed at $q = 0.013$, and maximum rainfall intensity did not differ significantly ($q = 0.263$). Extensive overlap among distributions indicates probabilistic hydrological context rather than discrete or deterministic controls.